

## Kinetics and Mechanisms of S(IV) Reductions of Bromite and Chlorite Ions

Kara E. Huff Hartz, Jeffrey S. Nicoson, Lu Wang, and Dale W. Margerum\*

Department of Chemistry, Purdue University, West Lafayette, Indiana 47907-1393

Received July 22, 2002

The reaction of bromite with aqueous S(IV) is first order in both reactants and is general-acid catalyzed. The reaction half-lives vary from 5 ms ( $p[H^+] 5.9$ ) to 210 s ( $p[H^+] 13.1$ ) for 0.7 mM excess S(IV) at 25 °C. The proposed mechanism includes a rapid reaction ( $k_1 = 3.0 \times 10^7 \text{ M}^{-1} \text{ s}^{-1}$ ) between  $\text{BrO}_2^-$  and  $\text{SO}_3^{2-}$  to form a steady-state intermediate,  $(\text{O}_2\text{BrSO}_3)^{3-}$ . General acids assist the removal of an oxide ion from  $(\text{O}_2\text{BrSO}_3)^{3-}$  to form  $\text{OBrSO}_3^-$ , which hydrolyzes rapidly to give  $\text{OBr}^-$  and  $\text{SO}_4^{2-}$ . Subsequent fast reactions between  $\text{HOBr/OBr}^-$  and  $\text{SO}_3^{2-}$  give  $\text{Br}^-$  and  $\text{SO}_4^{2-}$  as final products. In contrast, the chlorite reactions with S(IV) are 5–6 orders of magnitude slower. These reactions are specific-acid, not general-acid, catalyzed. In the proposed mechanism,  $\text{ClO}_2^-$  and  $\text{SO}_3\text{H}^-/\text{SO}_2$  react to form  $(\text{OCIOSO}_3\text{H})^{2-}$  and  $(\text{OCIOSO}_2)^-$  intermediates which decompose to form  $\text{OCl}^-$  and  $\text{SO}_4^{2-}$ . Subsequent fast reactions between  $\text{HOCl/OCl}^-$  and S(IV) give  $\text{Cl}^-$  and  $\text{SO}_4^{2-}$  as final products.  $\text{SO}_2$  is 6 orders of magnitude more reactive than  $\text{SO}_3\text{H}^-$ , where  $k_5(\text{SO}_2/\text{ClO}_2^-) = 6.26 \times 10^6 \text{ M}^{-1} \text{ s}^{-1}$  and  $k_6(\text{SO}_3\text{H}^-/\text{ClO}_2^-) = 5.5 \text{ M}^{-1} \text{ s}^{-1}$ . Direct reaction between  $\text{ClO}_2^-$  and  $\text{SO}_3^{2-}$  is not observed. The presence or absence of general-acid catalysis leads to the proposal of different connectivities for the initial reactive intermediates, where a Br–S bond forms with  $\text{BrO}_2^-$  and  $\text{SO}_3^{2-}$ , while an O–S bond forms with  $\text{ClO}_2^-$  and  $\text{SO}_3\text{H}^-$ .

## Introduction

The mechanisms of the hypohalous acid ( $\text{HOX}$ ,  $X = \text{Cl}$  or  $\text{Br}$ ) reduction with many nucleophiles ( $\text{I}^-$ ,  $\text{NO}_2^-$ ,  $\text{SO}_3^{2-}$ ,  $\text{Br}^-$ ,  $\text{CN}^-$ ,  $\text{ClO}_2^-$ ) proceed by halogen(I) transfer to the nucleophile with halide release.<sup>1</sup> However, little is known about the reaction mechanisms for the reduction of halite ions ( $\text{XO}_2^-$ ). This is due in part to the instability of aqueous halite ions (chlorite and bromite are stable only in basic solution, and iodite is a transient species) and due to the lack of commercially available bromite salts. Halites are often encountered in oscillating reactions,<sup>2</sup> and bromite is an intermediate for bromate ion formation in the disinfection of drinking water.<sup>3</sup> Bromate is a carcinogen, and the USEPA

has set the maximum contaminant level for drinking water at  $10 \mu\text{g L}^{-1} \text{ BrO}_3^-$ .<sup>4</sup>

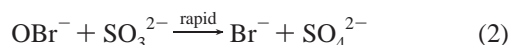
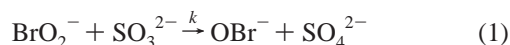
Lee and Lister<sup>5</sup> reported the kinetics of the reaction between bromite and sulfite in basic solutions. They observed kinetics that were first order in bromite and in sulfite and proposed that the reaction proceeds by two stages (eqs 1 and 2). They found the rate expression in eq 3 for the reaction where  $[\text{OH}^-] = 0.016\text{--}0.046 \text{ M}$ ,  $k_a = 3.73 \text{ M}^{-1} \text{ s}^{-1}$  and  $k_b = 0.121 \text{ s}^{-1}$  at 25.0 °C, and  $\mu = 1.0 \text{ M}$ . They assigned the  $k_a$  pathway to a direct reaction of  $\text{BrO}_2^-$  and  $\text{SO}_3^{2-}$  and the  $k_b$  pathway to a reaction between  $\text{HBrO}_2$  and  $\text{SO}_3^{2-}$  and proposed that the reaction proceeds by a simple oxygen-atom transfer mechanism. In our work, we measure the kinetics of  $\text{BrO}_2^-/\text{S(IV)}$  reactions over an extended  $p[H^+]$  range. We show the strong effects of buffers and pH on the  $\text{BrO}_2^-/\text{S(IV)}$  reaction rates and propose a mechanism to account for these effects.

\* To whom correspondence should be addressed. E-mail: margerum@purdue.edu.

(1) (a) Kumar, K.; Day, R. A.; Margerum, D. W. *Inorg. Chem.* **1986**, *25*, 4344–4350. (b) Kumar, K.; Margerum, D. W. *Inorg. Chem.* **1987**, *26*, 2706–2711. (c) Fogelman, K. D.; Walker, D. M.; Margerum, D. W. *Inorg. Chem.* **1989**, *28*, 986–993. (d) Gerritsen, C. M.; Margerum, D. W. *Inorg. Chem.* **1990**, *29*, 2757–2762. (e) Troy, R. C.; Margerum, D. W. *Inorg. Chem.* **1991**, *30*, 3538–3543. (f) Johnson, D. W.; Margerum, D. W. *Inorg. Chem.* **1991**, *30*, 4845–4850. (g) Gerritsen, C. M.; Gazda, M.; Margerum, D. W. *Inorg. Chem.* **1993**, *32*, 5739–5748. (h) Furman, C. S.; Margerum, D. W. *Inorg. Chem.* **1998**, *37*, 4321–4327. (i) Jia, Z.; Margerum, D. W.; Francisco, J. S. *Inorg. Chem.* **2000**, *39*, 2614–2620.

(2) (a) Orbán, M.; Epstein, I. R. *J. Phys. Chem.* **1995**, *99*, 2358–2362. (b) Faria, R. D.; Lengyel, I.; Epstein, I. R. *J. Phys. Chem.* **1993**, *97*, 1164–1171. (c) De Kepper, P.; Boissonade, J.; Epstein, I. *J. Phys. Chem.* **1990**, *94*, 6525–6536. (3) von Gunten, U.; Oliveras, Y. *Environ. Sci. Technol.* **1998**, *32*, 63–70. (4) *Fed. Regist.* **1998**, *63*, 69390. (5) Lee, C. L.; Lister, M. W. *Can. J. Chem.* **1979**, *57*, 1524–1530.

#### S(IV) Reductions of Bromite and Chlorite Ions



$$\frac{-d[\text{BrO}_2^-]}{dt} = k[\text{BrO}_2^-][\text{SO}_3^{2-}] \quad k = k_a + \frac{k_b}{[\text{OH}^-]} \quad (3)$$

The corresponding chlorite/S(IV) reaction has been studied somewhat more than the bromite/S(IV) reaction. Halperin and Taube<sup>6</sup> stated that the reaction is essentially complete within 1 min in 0.1 M HCl and at pH 5. They suggested that the reaction proceeds by oxygen-atom transfer. Adam and Gordon<sup>7</sup> used basic sulfite solutions (pH > 10.5) to remove hypochlorite selectively from chlorite solutions at room temperature for subsequent titration and chromatographic analysis. This indicates that the chlorite/sulfite reaction is relatively slow at this pH. Nagypál et al.<sup>8</sup> found the  $\text{ClO}_2^-/\text{SO}_3^{2-}$  reaction is complete within a few seconds at 90 °C in a continuous-stirred-tank reactor above pH 12. Frerichs et al.<sup>9</sup> gave rate constants at 25 °C for the three pathways in eqs 4–6. These are from the unpublished data of Rushing and Thompson. In our work, we see no contribution from rate 1 (eq 4) and find different values for rates 2 and 3 for the  $\text{ClO}_2^-/\text{S(IV)}$  reaction. Furthermore, we show buffers have no effect on the  $\text{ClO}_2^-/\text{S(IV)}$  reaction rates.

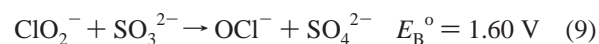
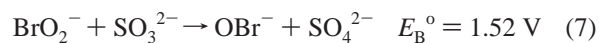
$$\text{rate 1} = k_1'[\text{ClO}_2^-][\text{SO}_3^{2-}] \quad k_1' = 1.2 \times 10^{-2} \text{ M}^{-1} \text{ s}^{-1} \quad (4)$$

$$\text{rate 2} = k_2'[\text{ClO}_2^-][\text{SO}_3\text{H}^-] \quad k_2' = 24.7 \text{ M}^{-1} \text{ s}^{-1} \quad (5)$$

$$\text{rate 3} = k_3'[\text{ClO}_2^-][\text{H}^+][\text{SO}_3\text{H}^-] \\ k_3' = 2.19 \times 10^8 \text{ M}^{-2} \text{ s}^{-1} \quad (6)$$

The electrode potentials in basic solution for the two-step reduction of  $\text{BrO}_2^-$  and  $\text{ClO}_2^-$  by  $\text{SO}_3^{2-}$  are shown in eqs 7–10.<sup>10</sup> The  $\text{BrO}_2^-/\text{OBr}^-$  potential is calculated on the basis of the  $\text{BrO}_3^-/\text{OBr}^-$ ,<sup>10</sup>  $\text{BrO}_2^-/\text{BrO}_3^-$ ,<sup>11</sup> and  $\text{BrO}_2^-/\text{BrO}_2^-$  couples. The thermodynamic driving forces for the  $\text{BrO}_2^-/\text{SO}_3^{2-}$  and the  $\text{ClO}_2^-/\text{SO}_3^{2-}$  reactions are comparable. Our work shows that despite the similarities in the reaction potentials and products, the  $\text{BrO}_2^-/\text{S(IV)}$  reactions are more than 5 orders of magnitude faster than the  $\text{ClO}_2^-/\text{S(IV)}$  reactions. The reaction kinetics suggest that  $\text{BrO}_2^-/\text{S(IV)}$  reactions and  $\text{ClO}_2^-/\text{S(IV)}$  reactions occur by different pathways. Reaction mechanisms are proposed to account for

these effects, and the reactions of oxybromine anions ( $\text{OBr}^-$ ,  $\text{BrO}_2^-$ , and  $\text{BrO}_3^-$ ) and oxychlorine anions ( $\text{OCl}^-$ ,  $\text{ClO}_2^-$ , and  $\text{ClO}_3^-$ ) with S(IV) are compared and contrasted.



#### Experimental Section

**Reagents.** All solutions were prepared using distilled, dionized (18 MΩ cm) water that was boiled to remove  $\text{CO}_2$  and sparged with  $\text{Ar(g)}$  to remove dissolved oxygen.  $\text{NaClO}_4$  was recrystallized before use and standardized gravimetrically. Carbonate-free NaOH was standardized against potassium hydrogen phthalate.  $\text{Na}_2\text{SO}_3$  solutions (>98.5%) were prepared just before use and were standardized by iodimetry.<sup>13</sup> Several techniques were utilized to exclude oxygen from the sulfite solutions: sonication of solutions for the dissolution of the solid salt; continuous  $\text{Ar(g)}$  sparging; transfer of solutions by gastight syringes.  $\text{NaClO}_2$  was recrystallized<sup>1h,14</sup> and standardized spectrophotometrically, where  $\epsilon_{260} = 154 \text{ M}^{-1} \text{ cm}^{-1}$ .<sup>1h</sup> The previously reported<sup>12</sup> synthesis of sodium bromite was modified (by more careful cleanup methods) to give improved purity with 63%  $\text{NaBrO}_2$  (by weight), 14% NaOH, 1.9%  $\text{Na}_2\text{SO}_4$ , <0.08%  $\text{NaNO}_3$ , 7.0%  $\text{NaBrO}_3$ , 1.3% NaBr, and waters of crystallization. The hydroxide content of the bromite salt was measured by adding  $\text{Na}_2\text{HPO}_4$  to a bromite stock and measuring the resulting  $\text{p[H}^+]$  change caused by  $\text{OH}^-$  reaction with  $\text{HPO}_4^{2-}$ . Sulfate, nitrate, bromate, and bromide have no effect on the observed kinetics under the conditions of the experiments. Bromite solutions were standardized spectrophotometrically, where  $\epsilon_{295} = 115 \text{ M}^{-1} \text{ cm}^{-1}$ .<sup>15</sup>

**Methodology and Instrumentation.** The measured pH was converted to  $\text{p[H}^+]$  on the basis of electrode calibration at  $\mu = 1.0 \text{ M}$  ( $\text{NaClO}_4$ ). Ion chromatographic data were obtained with a Dionex DX-500 instrument as described previously.<sup>12</sup> UV–vis spectra and kinetic scans were obtained on a Perkin-Elmer Lambda-9 UV–vis–NIR spectrophotometer. Quartz cells were used and were thermostated at 25.0(1) °C. Data for faster reactions were obtained on an Applied Photophysics stopped-flow spectrometer, equipped with a 0.962 cm path length cell. At least 10 pushes/reaction were averaged for analysis, and SigmaPlot v. 8.0<sup>16</sup> was used for data analysis. Observed first-order rate constants ( $k_{\text{obs}}$ ) greater than  $50 \text{ s}^{-1}$  were corrected for mixing according to eq 11, where  $k_{\text{corr}}$  = corrected rate constant and  $k_{\text{mix}} = 4620(120) \text{ s}^{-1}$ .<sup>17</sup>

$$k_{\text{corr}} = \left( \frac{1}{k_{\text{obs}}} - \frac{1}{k_{\text{mix}}} \right)^{-1} \quad (11)$$

The halite/sulfite reaction rates were measured when the  $[\text{S(IV)}]/[\text{XO}_2^-]$  ratio was greater than 20/1 to maintain pseudo-first-order conditions. The loss of bromite was followed at 295 nm ( $\epsilon = 115$

(6) Halperin, J.; Taube, H. *J. Am. Chem. Soc.* **1952**, *74*, 375–380.

(7) Adam, L. C.; Gordon, G. *Anal. Chem.* **1995**, *67*, 535–540.

(8) Nagypál, I. R.; Epstein, I.; Kustin, K. *Int. J. Chem. Kinet.* **1986**, *18*, 345–353.

(9) Frerichs, G. A.; Mlnarik, T. M.; Grun, R. J.; Thompson, R. C. *J. Phys. Chem. A* **2001**, *105*, 829–837.

(10) *Standard Potentials in Aqueous Solutions*; Bard, A. J., Parsons, R., Jordan, J., Eds.; Marcel Dekker: New York, 1985; pp 74–75, 79–82, 102.

(11) Stanbury, D. M. In *Advances in Inorganic Chemistry*; Sykes, A. G., Ed.; Academic Press: San Diego, CA, 1989; Vol. 33, pp 69–137.

(12) Wang, L.; Nicoson, J. S.; Huff Hartz, K. E.; Fransisco, J. S.; Margerum, D. W. *Inorg. Chem.* **2002**, *41*, 108–113.

(13) Jeffery, G. H.; Bassett, J.; Mendham, J.; Denney, R. C. *Vogel's Textbook of Quantitative Chemical Analysis*, 5th ed.; Longman Scientific & Technical: Essex, U.K., 1980; pp 384–398.

(14) Peintler, G.; Nagypál, I.; Epstein, I. R. *J. Phys. Chem.* **1990**, *94*, 2954–2958.

(15) (a) Lee, C. L.; Lister, M. W. *Can. J. Chem.* **1971**, *49*, 2822–2826. (b) Perrone, T. F. Ph.D. Thesis, Purdue University, 1999; pp 89–91.

(16) *SigmaPlot v. 8.0 for Windows*; SPSS Inc.: Chicago, IL, 2002.

(17) Nicoson, J. S.; Margerum, D. W. *Inorg. Chem.* **2002**, *41*, 342–347.

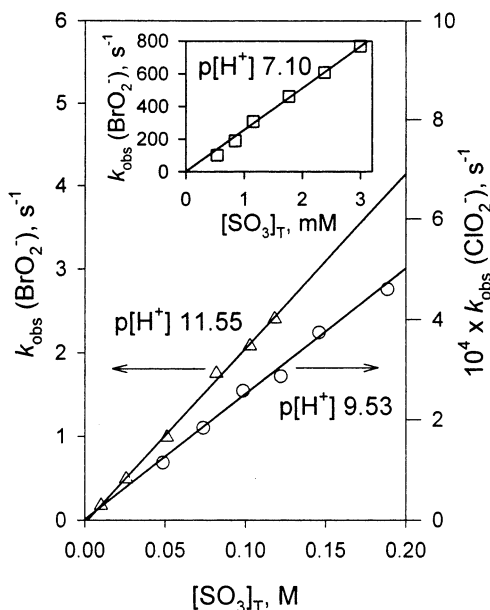


**Figure 1.** Sulfite dependence of the halite/S(IV) reaction where  $k_{\text{obs}} = \text{slope}[\text{SO}_3]_{\text{T}}$  ( $y$ -intercepts are zero within the error): ( $\Delta$ ) bromite data where slope from fit equals  $20.9(5) \text{ M}^{-1} \text{ s}^{-1}$ ; ( $\circ$ ) chlorite data where slope from fit equals  $2.5(1) \times 10^{-3} \text{ M}^{-1} \text{ s}^{-1}$ . Conditions:  $0.659 \text{ mM BrO}_2^-$ ,  $30.0 \text{ mM [PO}_4]_{\text{T}}$ ,  $\text{p[H}^+] 11.55(3)$ ;  $4.0 \text{ mM ClO}_2^-$ ,  $50 \text{ mM [CO}_3]_{\text{T}}$ ,  $\text{p[H}^+] 9.53(3)$ ,  $\mu = 1.0 \text{ M}$ ,  $25.0(1) \text{ }^\circ\text{C}$ . Insert shows  $k_{\text{obs}}$  dependence on  $[\text{SO}_3]_{\text{T}}$  for the bromite/sulfite reaction ( $\square$ ) at lower  $\text{p[H}^+]$ . Slope =  $2.56(5) \times 10^5 \text{ M}^{-1} \text{ s}^{-1}$ . Conditions:  $0.075 \text{ mM BrO}_2^-$ ,  $40 \text{ mM [PO}_4]_{\text{T}}$ ,  $\text{p[H}^+] 7.10(1)$ .

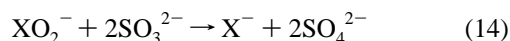
$\text{M}^{-1} \text{ cm}^{-1}$ )<sup>15</sup> or  $240 \text{ nm}$  ( $\epsilon = 620 \text{ M}^{-1} \text{ cm}^{-1}$ ). The loss of chlorite was followed at  $260 \text{ nm}$  ( $\epsilon = 154 \text{ M}^{-1} \text{ cm}^{-1}$ )<sup>1h</sup> or  $290 \text{ nm}$  ( $\epsilon = 97 \text{ M}^{-1} \text{ cm}^{-1}$ ); this wavelength was used when  $\text{SO}_3^{2-}$  absorbance overwhelms the  $\text{ClO}_2^-$  signal. The rates of loss of bromite and chlorite were first order (eq 12), and the data fit an integrated rate expression (eq 13), where  $k_{\text{obs}}$  = observed rate constant,  $A$  = absorbance,  $t$  = time,  $i$  = initial, and  $\infty$  = final.

$$\frac{-d[\text{XO}_2^-]}{dt} = k_{\text{obs}}[\text{XO}_2^-] \quad (12)$$

$$A_t = A_\infty + (A_i - A_\infty)e^{-k_{\text{obs}}t} \quad (13)$$

## Results and Discussion

**Stoichiometry and Reaction Order with Respect to Halite and Sulfite.** Ion chromatography and UV-vis absorbance spectrometry were used to verify the reaction stoichiometries. Bromide and sulfate are the only products observed from the bromite/S(IV) reaction, and chloride and sulfate are the only products observed from the chlorite/S(IV) reaction. For the  $\text{BrO}_2^-/\text{S(IV)}$  reaction, the average ratio of initial  $[\text{BrO}_2^-]$  to final  $[\text{Br}^-]$  is  $1.01(2)$  (after  $[\text{Br}^-]$  from the bromite stock is subtracted). For the  $\text{ClO}_2^-/\text{S(IV)}$  reaction, the average ratio of initial  $[\text{ClO}_2^-]$  to final  $[\text{Cl}^-]$  is  $1.03(5)$ . The stoichiometry for the four-electron reduction of halite by sulfite is given by eq 14.



The sulfite concentration was varied to establish the reaction order in  $[\text{SO}_3]_{\text{T}}$  where  $[\text{SO}_3]_{\text{T}} = [\text{SO}_3\text{H}^-] + [\text{SO}_3^{2-}] + [\text{SO}_2]$ . The reactions of halites with sulfite are first order

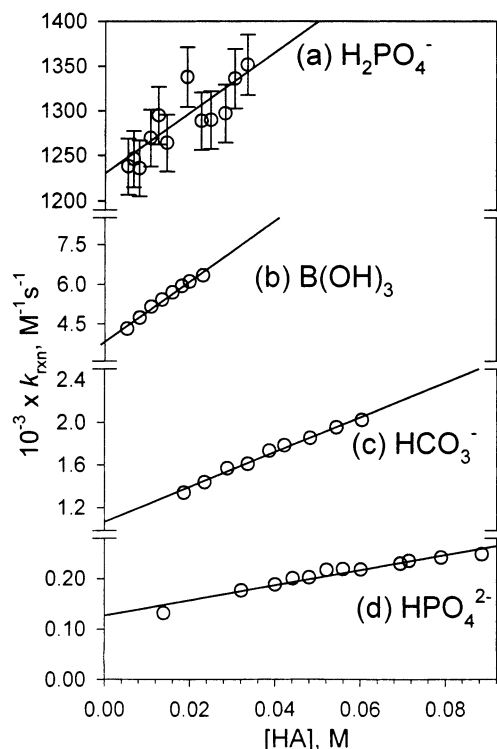
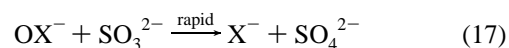
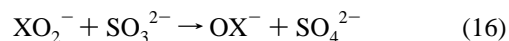


**Figure 2.** Buffer dependence of  $\text{BrO}_2^-/\text{SO}_3^{2-}$  reaction. (a)  $\text{H}_2\text{PO}_4^-$  data are corrected for  $[\text{SO}_3\text{H}^-]$  by  $k_{\text{rxn}}(K_a(\text{SO}_3\text{H}^-) + [\text{H}^+])/K_a(\text{SO}_3\text{H}^-)$ . Conditions:  $0.105 \text{ mM BrO}_2^-$ ,  $0.921 \text{ mM S(IV)}$ ,  $\text{p[H}^+] 6.59(3)$ , slope =  $3.4(7) \times 10^6 \text{ M}^{-2} \text{ s}^{-1}$ . Error bars reflect the standard deviation in determination. (b)  $\text{B(OH)}_3$  data are corrected for boric acid/sulfite complex by eq 21. Conditions:  $0.50 \text{ mM BrO}_2^-$ ,  $6.08(4) \text{ mM S(IV)}$ ,  $\text{p[H}^+] 8.98(2)$ , slope =  $1.06(5) \times 10^5 \text{ M}^{-2} \text{ s}^{-1}$ . (c)  $\text{HCO}_3^-$  conditions:  $0.96 \text{ mM BrO}_2^-$ ,  $30.8(2) \text{ mM S(IV)}$ ,  $\text{p[H}^+] 9.53(1)$ , slope =  $1.50(6) \times 10^4 \text{ M}^{-2} \text{ s}^{-1}$ . (d)  $\text{HPO}_4^{2-}$  conditions:  $0.80 \text{ mM BrO}_2^-$ ,  $30.7(2) \text{ mM S(IV)}$ ,  $\text{p[H}^+] 10.48(2)$ , slope =  $1.5(2) \times 10^3 \text{ M}^{-2} \text{ s}^{-1}$ .

in  $[\text{SO}_3]_{\text{T}}$  (Figure 1), and the rate expression for the halite/S(IV) reaction is shown in eq 15.

$$\frac{-d[\text{XO}_2^-]}{dt} = k_{\text{rxn}}[\text{XO}_2^-][\text{SO}_3]_{\text{T}} \quad k_{\text{rxn}} = \frac{k_{\text{obs}}}{[\text{SO}_3]_{\text{T}}} \quad (15)$$

The first-order dependences in  $[\text{XO}_2^-]$  and  $[\text{SO}_3]_{\text{T}}$  indicate that the rate-determining steps involve the reduction of halite to hypohalite (eq 16). The  $\text{HOCl}/\text{OCl}^-$  reactions with sulfite<sup>1c</sup> and the  $\text{HOBr}/\text{OBr}^-$  reactions with sulfite<sup>1e</sup> are known to be much faster than the measured reaction rates. Therefore, subsequent hypohalite reduction (eq 17) is not observed kinetically.



**Buffer Dependence of the  $\text{BrO}_2^-/\text{SO}_3^{2-}$  Reaction.** The rate constants for the  $\text{BrO}_2^-/\text{SO}_3^{2-}$  reaction increase with increasing phosphate ( $[\text{PO}_4]_{\text{T}}$ ), carbonate ( $[\text{CO}_3]_{\text{T}}$ ), and borate ( $[\text{Bor}]_{\text{T}}$ ) buffer concentration, where acidic forms of the buffers accelerate the reaction. Plots of  $k_{\text{rxn}}$  vs the acidic form of the buffer (HA) are given in Figure 2, where the  $\text{HPO}_4^{2-}$ ,  $\text{HCO}_3^-$ , and  $\text{H}_2\text{PO}_4^-$  concentrations are calculated from the corresponding acid dissociation constants ( $K_a(\text{HPO}_4^{2-}) =$

#### S(IV) Reductions of Bromite and Chlorite Ions

$10^{-11.08}$  M,  $K_a(\text{HCO}_3^-) = 10^{-9.57}$  M,  $K_a(\text{H}_2\text{PO}_4^-) = 10^{-6.26}$  M).<sup>1h,18,19a</sup> The reaction rate increases linearly as the concentration of the general acid increases.

Borate buffer also affects the rate of  $\text{BrO}_2^-/\text{S(IV)}$  reaction. Boric acid is known to form complexes with several oxyanions, including  $\text{OCl}^-$ ,  $\text{OBr}^-$ , and  $\text{NO}_2^-$ .<sup>20</sup> For this reason, bromite and sulfite solutions were examined for boric acid complex formation. Spectral scans showed no shift in the bromite spectrum upon addition of borate buffer ( $\text{p}[\text{H}^+] = 8.6$ ) so that bromite/boric acid complex formation appears to be negligible. However, boric acid causes the sulfite absorbance to decrease, due to the formation of a complex. A boric acid/sulfite complex equilibrium constant ( $K^{\text{BS}}$ ) is defined as shown in eq 18.



$$A_T = b(\epsilon^{\text{S}}[\text{SO}_3^{2-}] + \epsilon^{\text{HS}}[\text{SO}_3\text{H}^-] + \epsilon^{\text{BS}}[(\text{SO}_3\text{B(OH)}_3)^{2-}]) \quad (19)$$

The  $K^{\text{BS}}$  value is calculated from absorbance data on the basis of eq 19 for total absorbance ( $A_T$ ) at any wavelength, where  $b = 0.10$  cm path length and  $\epsilon =$  molar absorptivities of S (sulfite), HS (hydrogen sulfite), and BS (boric acid/sulfite complex), respectively. The absorbance of  $\text{SO}_3\text{H}^-$  is negligible above 230 nm,<sup>21</sup> and the measured absorbances were corrected for the small borate buffer and  $\text{NaClO}_4$  absorbance. Equation 20 is derived by incorporating the equation for total

$$A_T = \frac{(\epsilon^{\text{S}} + \epsilon^{\text{BS}}K^{\text{BS}}[\text{B(OH)}_3])bK_a(\text{SO}_3\text{H}^-)[\text{SO}_3]_{\text{T}}}{K_a(\text{HSO}_3^-) + [\text{H}^+] + K_a(\text{SO}_3\text{H}^-)K^{\text{BS}}[\text{B(OH)}_3]} \quad (20)$$

sulfite species ( $[\text{SO}_3]_{\text{T}} = [\text{SO}_3^{2-}] + [\text{SO}_3\text{H}^-] + [(\text{SO}_3\text{B(OH)}_3)^{2-}]$ ), eq 19, and the equilibrium constant between  $\text{SO}_3\text{H}^-$  and  $\text{SO}_3^{2-}$ . The concentration of  $\text{B(OH)}_3$  is calculated using  $K_a(\text{B(OH)}_3) = 10^{-8.85}$  M<sup>22a</sup> after correction for the formation of polyborates (see Supporting Information for details).<sup>22b</sup> The measured absorbances at three wavelengths (240, 245, and 250 nm) were curve fit to eq 20, where the calculated sulfite/boric acid equilibrium complex value is  $K^{\text{BS}} = 7.6(5)$  M<sup>-1</sup>. Midgely<sup>20</sup> developed a linear free-energy relationship for boric acid complexes with univalent ions ( $K$ ) on the basis of the  $\text{p}K_a$  value of the conjugate acid of the univalent ion ( $\log K = -2.15(58) + 0.45(5)\text{p}K_a$ ). The  $K^{\text{BS}}$  predicted by this equation is  $4.8(4)$  M<sup>-1</sup>, which is in reasonable agreement with the value obtained here. Midgely's equation also predicts (on the basis of  $\text{p}K_a(\text{HBrO}_2) = 3.59(5)$ , measured under the conditions of this experiment; see Figure S2) that the  $\text{BrO}_2^-/\text{B(OH)}_3$  complex formation constant ( $K^{\text{BB}}$ ) would be  $0.3(5)$  M<sup>-1</sup>. If this value were valid,

- (18) Tesfai, T. M.; Margerum, D. W. Unpublished work.  
 (19) Martell, A. E.; Smith, R. M. *Critical Stability Constants*; Plenum Press: New York, 1982; Vol. 5, (a) p 403, (b) p 411.  
 (20) (a) Bousher, A.; Brimblecombe, P.; Midgely, D. *J. Chem. Soc., Dalton Trans.* **1987**, 943–946. (b) Midgely, D. *J. Chem. Soc., Dalton Trans.* **1991**, 1585–1587.  
 (21) Liu, Q. Ph.D. Thesis, Purdue University, 2000; p 99.  
 (22) (a) Paál, T.; Barcza, L. *Acta Chim. Acad. Sci. Hung.* **1975**, 78, 33–40. (b) Baes, C. F. Jr.; Mesmer, R. E. *The Hydrolysis of Cations*; John Wiley & Sons: New York, 1976; pp 104–111.

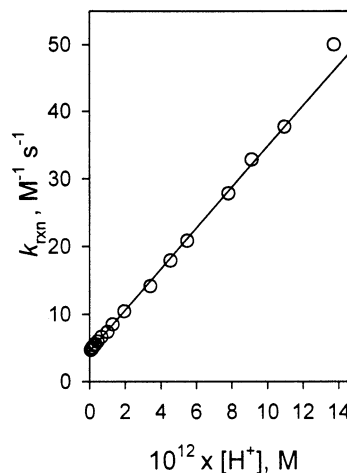


**Figure 3.**  $[\text{H}^+]$  dependence of the  $\text{BrO}_2^-/\text{SO}_3^{2-}$  reaction in absence of buffers,  $7.7 \times 10^{-14}$ – $1.4 \times 10^{-11}$  M  $\text{H}^+$ ,  $\mu = 1.0$  M, and  $25.0(1)$  °C: intercept =  $4.50(3)$  M<sup>-1</sup> s<sup>-1</sup>; slope =  $3.03(4) \times 10^{12}$  M<sup>-2</sup> s<sup>-1</sup>.

no more than 1% of  $\text{BrO}_2^-$  would be complexed to  $\text{B(OH)}_3$ . This may explain why no  $\text{BrO}_2^-/\text{B(OH)}_3$  complex is observed spectrophotometrically.

Borate buffer accelerates the bromite/sulfite reaction but also simultaneously decreases the rate because a fraction of  $[\text{SO}_3]_{\text{T}}$  is sequestered as the unreactive  $(\text{SO}_3\text{B(OH)}_3)^{2-}$  species. For this reason,  $k_{\text{rxn}}$  must be corrected for  $K^{\text{BS}}$  as well as  $K_a(\text{SO}_3\text{H}^-)$  (eq 21). With this correction,  $k_{\text{rxn}}$  increases linearly with increasing  $[\text{B(OH)}_3]$  (Figure 2).

Hydrogen sulfite ( $\text{SO}_3\text{H}^-$ ,  $\text{p}K_a = 6.30(5)$ )<sup>23</sup> also acts as a general acid and has an acid strength similar to that of  $\text{H}_2\text{PO}_4^-$  ( $\text{p}K_a = 6.26$ ). Under our conditions, however, the concentration of  $\text{SO}_3\text{H}^-$  is low relative to that of  $\text{H}_2\text{PO}_4^-$ , and so the  $\text{SO}_3\text{H}^-$  contribution to the general-acid-catalyzed rate is negligible.

$$k_{\text{rxn}} = \frac{k_{\text{obs}} (K_a(\text{SO}_3\text{H}^-) + [\text{H}^+] + K_a(\text{SO}_3\text{H}^-)K^{\text{BS}}[\text{B(OH)}_3])}{[\text{SO}_3]_{\text{T}} K_a(\text{SO}_3\text{H}^-)} \quad (21)$$

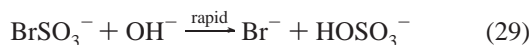
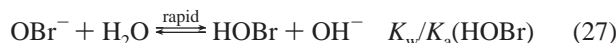
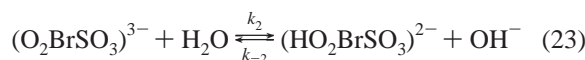
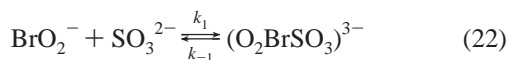
**$[\text{H}^+]$  Dependence of the  $\text{BrO}_2^-/\text{SO}_3^{2-}$  Reaction.** The  $[\text{H}^+]$  concentration was varied by adding different amounts of NaOH to  $\text{BrO}_2^-$  solutions and observing the reaction with  $\text{SO}_3^{2-}$ . A plot of  $k_{\text{rxn}}$  vs  $[\text{H}^+]$  is shown in Figure 3. The plot is linear in the range of  $7.7 \times 10^{-14}$ – $1.4 \times 10^{-11}$  M  $\text{H}^+$ . The intercept and slope of this plot are  $4.50(3)$  M<sup>-1</sup> s<sup>-1</sup> and  $3.03(4) \times 10^{12}$  M<sup>-2</sup> s<sup>-1</sup>, respectively. The  $[\text{H}^+]$  dependences were also resolved in  $\text{HPO}_4^{2-}/\text{PO}_4^{3-}$ ,  $\text{HCO}_3^-/\text{CO}_3^{2-}$ , and borate buffers, and the slopes were in agreement, after correction for the buffer acid contribution, from  $3.7 \times 10^{-12}$  to  $1.6 \times 10^{-8}$  M  $\text{H}^+$ .

The intercept in Figure 3 is equivalent to Lee and Lister's<sup>5</sup> definition of  $k_a$ , and the slope multiplied by  $K_w$  ( $10^{-13.60}$  M<sup>2</sup>,  $\mu = 1.0$  M  $\text{NaClO}_4$ )<sup>24</sup> corresponds to  $k_b$  in eq 3. Our  $[\text{H}^+]$  range is larger by many orders of magnitude than they<sup>5</sup> used,

- (23) Van Eldik, R.; Harris, G. *Inorg. Chem.* **1980**, 19, 880–886.  
 (24) Molina, M.; Melios, C.; Tognolli, J. O.; Luchiarri, L. C.; Jafellicci, M., Jr. *J. Electroanal. Chem. Interfacial Electrochem.* **1979**, 105, 237–246.

and we find  $k_a = 4.50 \text{ M}^{-1} \text{ s}^{-1}$  and  $k_b = 0.076 \text{ s}^{-1}$ . The fraction of protonated bromite can be neglected because the  $pK_a$  of bromous acid is 3.59(5).

**BrO<sub>2</sub><sup>-</sup>/SO<sub>3</sub><sup>2-</sup> Reaction Mechanism.** The kinetic dependence on BrO<sub>2</sub><sup>-</sup>, SO<sub>3</sub><sup>2-</sup>, and HA requires reaction intermediates that lead to the reduction of Br(III) and the oxidation of S(IV). Electron transfer processes via Br(II) and S(V) would be extremely unfavorable and are ruled out. Hence, a (BrO<sub>2</sub>·SO<sub>3</sub>)<sup>3-</sup> intermediate must form that can react with general acids to cause Br(III) reduction and S(IV) oxidation. However, a preequilibrium between HA and bromite or HA and sulfite (except B(OH)<sub>3</sub>, which complexes SO<sub>3</sub><sup>2-</sup>) is not acceptable because this mechanism would lead to specific-acid, not general-acid, catalysis. Therefore, bromite and sulfite, not HBrO<sub>2</sub> or SO<sub>3</sub>H<sup>-</sup>, are the reactive species in BrO<sub>2</sub><sup>-</sup>/S(IV) reactions. The mechanism of eqs 22–29 is proposed. Bromite acts as an electrophile and reacts rapidly with sulfite, a nucleophile, to form (O<sub>2</sub>BrSO<sub>3</sub>)<sup>3-</sup>. This species can protonate to form (HO<sub>2</sub>BrSO<sub>3</sub>)<sup>2-</sup>. Kinetic and spectral data indicate that the concentrations of the (O<sub>2</sub>BrSO<sub>3</sub>)<sup>3-</sup> and (HO<sub>2</sub>BrSO<sub>3</sub>)<sup>2-</sup> are not appreciable. Reactions in carbonate, borate, and phosphate buffers (where  $p[H^+] > 7.2$ ) indicate that  $k_{-1} \gg k_3^{HA}[HA]$  and  $k_{-2}[OH^-] \gg k_4^{HA}[HA]$ . Hence, in the presence of buffers at  $p[H^+] > 7.2$ , (O<sub>2</sub>BrSO<sub>3</sub>)<sup>3-</sup> and (HO<sub>2</sub>BrSO<sub>3</sub>)<sup>2-</sup> can be treated as preequilibrium species.



We propose that general acids react with both adducts; HA removes O<sup>2-</sup> from (O<sub>2</sub>BrSO<sub>3</sub>)<sup>3-</sup> and releases OH<sup>-</sup>, whereas HA abstracts OH<sup>-</sup> from (HO<sub>2</sub>BrSO<sub>3</sub>)<sup>2-</sup> and releases H<sub>2</sub>O. The result in both cases would be an intermediate, OBrSO<sub>3</sub><sup>-</sup>, that rapidly hydrolyzes to form OBr<sup>-</sup>, HOSO<sub>3</sub><sup>-</sup>, and H<sup>+</sup>. In this process, Br(III) is reduced to Br(I) and S(IV) is oxidized to S(VI) during either the formation or hydrolysis of OBrSO<sub>3</sub><sup>-</sup>. The OBr<sup>-</sup> released is in rapid equilibrium with HOBr. The resulting HOBr reacts very rapidly with an additional SO<sub>3</sub><sup>2-</sup> to form BrSO<sub>3</sub><sup>-</sup> by a Br-atom transfer mechanism ( $k(\text{HOBr}/\text{SO}_3^{2-}) = 10^9 \text{ M}^{-1} \text{ s}^{-1}$ ).<sup>1c</sup> Finally, BrSO<sub>3</sub><sup>-</sup> rapidly hydrolyzes to form Br<sup>-</sup> and HOSO<sub>3</sub><sup>-</sup> which, under the experimental conditions, gives SO<sub>4</sub><sup>2-</sup> and H<sup>+</sup>. The  $pK_a$  of HOSO<sub>3</sub><sup>-</sup> is 1.10.<sup>19b</sup>

The expression for  $k_{\text{rxn}}$  on the basis of this mechanism, in the absence of buffers, is shown in eq 30, where  $K_1 = k_1/k_{-1}$  and  $K_2 = k_2/k_{-2}$ . The zero-order and first-order [H<sup>+</sup>] dependences of  $k_{\text{rxn}}$  are resolved from the data in Figure 3. The first-order dependence in [H<sup>+</sup>] is a combination of two pathways where  $(k_3^H K_1 + k_4^{H_2O} K_1 K_2 / K_w) = 3.03(4) \times 10^{12} \text{ M}^{-2} \text{ s}^{-1}$ . The intercept corresponds to a water-catalyzed pathway, where  $k_3^{H_2O} K_1 = 4.50(3) \text{ M}^{-1} \text{ s}^{-1}$ . The rate expression given by eq 30 includes a second-order dependence in [H<sup>+</sup>] (due to  $k_4^H$ ) that is not observed in the Figure 3. Therefore, the value for  $k_4^H K_1 K_2 / K_w$  must be less than  $5 \times 10^{17} \text{ M}^{-3} \text{ s}^{-1}$ . This pathway is not significant relative to the other paths when  $p[H^+] > 6.0$ .

$$k_{\text{rxn}} = \left[ k_3^{H_2O} K_1 + \left( k_3^H K_1 + \frac{k_4^{H_2O} K_1 K_2}{K_w} \right) [H^+] + \frac{k_4^H K_1 K_2}{K_w} [H^+]^2 \right] \frac{K_a(\text{SO}_3\text{H}^-)}{K_a(\text{SO}_3\text{H}^-) + [H^+]} \quad (30)$$

The presence of two bromite/sulfite intermediates, (O<sub>2</sub>BrSO<sub>3</sub>)<sup>3-</sup> and (HO<sub>2</sub>BrSO<sub>3</sub>)<sup>2-</sup>, and two general-acid-catalyzed paths are kinetic requirements. The composite rate constant for the first-order dependence in [H<sup>+</sup>] is  $3.03 \times 10^{12} \text{ M}^{-2} \text{ s}^{-1}$ . If the  $k_4^{H_2O}$  path did not exist, then  $k_3^H K_1 = 3.03 \times 10^{12} \text{ M}^{-2} \text{ s}^{-1}$ . The H<sub>3</sub>O<sup>+</sup>/(O<sub>2</sub>BrSO<sub>3</sub>)<sup>3-</sup> rate constant ( $k_3^H$ ) can be no greater than the diffusion control limit in aqueous solution,  $10^{10} \text{ M}^{-1} \text{ s}^{-1}$ . With this constraint, the lower limit for the formation constant of (O<sub>2</sub>BrSO<sub>3</sub>)<sup>3-</sup>,  $K_1$ , is  $303 \text{ M}^{-1}$ . With a formation constant this large, we would expect to observe a significant fraction of bromite complexed to sulfite. However, the kinetic spectra show no changes in the characteristic bromite peak shape, indicating that the (O<sub>2</sub>BrSO<sub>3</sub>)<sup>3-</sup> concentration is negligible and  $K_1 \leq 5 \times 10^{-3} \text{ M}^{-1}$ . Therefore, the second reaction pathway,  $k_4^{H_2O}$ , must occur. This path dominates the first-order dependence in [H<sup>+</sup>], so that  $k_4^{H_2O} K_1 K_2 / K_w = 3.03 \times 10^{12} \text{ M}^{-2} \text{ s}^{-1}$ , where  $k_3^H K_1 \leq 5 \times 10^7 \text{ M}^{-2} \text{ s}^{-1}$ .

Two general-acid-assisted pathways can be extracted from the experimental data,  $k_3^{HA} K_1$  and  $k_4^{HA} K_1 K_2 / K_w$ , and this is demonstrated for HCO<sub>3</sub><sup>-</sup>. Equation 31 shows the rate expression in carbonate buffer. At a fixed [H<sup>+</sup>], the equation becomes linear (eq 32) and the rate constant depends on [HCO<sub>3</sub><sup>-</sup>]. The slope of the  $k_{\text{rxn}}$  vs [HCO<sub>3</sub><sup>-</sup>] plot increases with increasing [H<sup>+</sup>], where the slope is the sum of the two HCO<sub>3</sub><sup>-</sup>-dependent paths (eq 33).

$$k_{\text{rxn}} = k_3^{H_2O} K_1 + \frac{k_4^{H_2O} K_1 K_2}{K_w} [H^+] + k_3^{HCO_3^-} K_1 [HCO_3^-] + \frac{k_4^{HCO_3^-} K_1 K_2}{K_w} [HCO_3^-] [H^+] \quad (31)$$

$$k_{\text{rxn}} = \text{intercept} + \text{slope} [HCO_3^-] \quad (32)$$

$$\text{slope} = k_3^{HCO_3^-} K_1 + \frac{k_4^{HCO_3^-} K_1 K_2}{K_w} [H^+] \quad (33)$$

**S(IV) Reductions of Bromite and Chlorite Ions**

**Table 1.** Summary of Equilibrium and Rate Constants<sup>a</sup>

constant	value (std dev)
$pK_a(\text{H}_3\text{O}^+)$	$-1.74^{25c}$
$pK_a(\text{HClO}_2)$	$1.72(2)^{26}$
$pK_a(\text{HBrO}_2)$	$3.59(5)^b$
$pK_a(\text{SO}_2)$	$1.90(5)^{23}$
$pK_a(\text{SO}_3\text{H}^-)$	$6.30(5)^{23}$
$pK_a(\text{H}_2\text{PO}_4^-)$	$6.26(1)^{1h}$
$pK_a(\text{HOCl})$	$7.47(1)^{1d}$
$pK_a(\text{HOBr})$	$8.59(3)^{1g}$
$pK_a(\text{B}(\text{OH})_3)$	$8.85(1)^{22a}$
$pK_a(\text{HCO}_3^-)$	$9.57(3)^{19a}$
$pK_a(\text{HPO}_4^{2-})$	$11.08(1)^{18}$
$pK_w$	$13.60(1)^{24}$
$pK_a(\text{H}_2\text{O})$	$15.34(1)^c$
$K^{\text{BS}d}$	$7.6(5) \text{ M}^{-1} b$
$K^{\text{BB}d}$	$0.3(5) \text{ M}^{-1} e$
$K^{\text{S}f}$	$4.9(1)^{28}$
<b>BrO<sub>2</sub><sup>-</sup>/SO<sub>3</sub><sup>2-</sup> Reaction Rate Constants</b>	
$k_1(\text{BrO}_2^-/\text{SO}_3^{2-})$	$3.0(5) \times 10^7 \text{ M}^{-1} \text{ s}^{-1} b$
$k_3^{\text{H}_2\text{O}}K_1$	$4.50(3) \text{ M}^{-1} \text{ s}^{-1} b$
$k_4^{\text{H}_2\text{O}}K_1K_2/K_w$	$3.03(4) \times 10^{12} \text{ M}^{-2} \text{ s}^{-1} b$
$k_3^{\text{HPO}_4^{2-}}K_1$	$1.5(2) \times 10^3 \text{ M}^{-2} \text{ s}^{-1} b$
$k_3^{\text{HCO}_3^-}K_1$	$9(2) \times 10^3 \text{ M}^{-2} \text{ s}^{-1} b$
$k_4^{\text{HCO}_3^-}K_1K_2/K_w$	$1.8(3) \times 10^{13} \text{ M}^{-3} \text{ s}^{-1} b$
$k_4^{\text{B}(\text{OH})_3}K_1K_2/K_w$	$8.1(5) \times 10^{13} \text{ M}^{-3} \text{ s}^{-1} b$
$k_4^{\text{H}_2\text{PO}_4^-}K_1K_2/K_w$	$1.3(3) \times 10^{13} \text{ M}^{-3} \text{ s}^{-1} b$
<b>ClO<sub>2</sub><sup>-</sup>/S(IV) Reaction Rate Constants</b>	
$k_5(\text{ClO}_2^-/\text{SO}_2)$	$6.26(4) \times 10^6 \text{ M}^{-1} \text{ s}^{-1} b$
$k_6(\text{ClO}_2^-/\text{SO}_3\text{H}^-)$	$5.5(3) \text{ M}^{-1} \text{ s}^{-1} b$

<sup>a</sup> 25.0 °C,  $\mu = 1.0 \text{ M}$  (NaClO<sub>4</sub>). <sup>b</sup>This work. <sup>c</sup>Calculated on the basis of  $pK_a(\text{H}_2\text{O}) = -\log(K_w/55.5)$ . <sup>d</sup>Equilibrium constant for the formation of boric acid/sulfite complex ( $K^{\text{BS}}$ ) and boric acid/bromite complex ( $K^{\text{BB}}$ ). <sup>e</sup>Calculated on the basis of  $pK_a(\text{HBrO}_2)$  and ref 20. <sup>f</sup> $K^{\text{S}}$  represents the ratio between hydrogen sulfite isomers,  $[\text{HOSO}_2^-]/[\text{HSO}_3^-]$ .

A plot of the slopes of the  $\text{HCO}_3^-$  dependence data vs  $[\text{H}^+]$  resolves the two  $\text{HCO}_3^-$ -assisted paths, where  $k_3^{\text{HCO}_3^-}K_1 = 9(2) \times 10^3 \text{ M}^{-2} \text{ s}^{-1}$  and  $k_4^{\text{HCO}_3^-}K_1K_2/K_w = 1.8(3) \times 10^{13} \text{ M}^{-3} \text{ s}^{-1}$ . These data support the presence of two general-acid-assisted paths (eqs 24 and 25).

A similar treatment was applied to  $\text{B}(\text{OH})_3$  dependence data, where  $k_4^{\text{B}(\text{OH})_3}K_1K_2/K_w = 8.1(5) \times 10^{13} \text{ M}^{-3} \text{ s}^{-1}$ . The y-intercept for the plot of the slopes vs  $[\text{H}^+]$  was zero within the error of the fit, which means that the  $k_3^{\text{B}(\text{OH})_3}K_1$  term is negligible under these conditions. As  $[\text{H}^+]$  increases, the  $(\text{O}_2\text{BrSO}_3)^{3-}/(\text{HO}_2\text{BrSO}_3)^{2-}$  equilibrium constant ( $K_2$ ) favors higher  $[(\text{HO}_2\text{BrSO}_3)^{2-}]$ . Thus, the  $k_3^{\text{B}(\text{OH})_3}$  path does not contribute significantly to the rate constant.

The general-acid-catalyzed rate constants resolved from the data are shown in Table 1. As noted above, as the  $[\text{H}^+]$  increases, the  $k_3^{\text{HA}}$  term becomes negligible. For this reason, we can assume that the  $k_3^{\text{H}_2\text{PO}_4^-}K_1$  term is negligible, and the  $k_4^{\text{H}_2\text{PO}_4^-}K_1K_2/K_w$  term is obtained from the curve fit of the  $k_{\text{rxn}}$  vs  $\text{H}_2\text{PO}_4^-$  data ( $1.3(3) \times 10^{13} \text{ M}^{-3} \text{ s}^{-1}$ ). By a similar argument, at lower  $[\text{H}^+]$ , the  $k_4^{\text{HPO}_4^{2-}}K_1K_2/K_w$  term is negligible, so that  $k_3^{\text{HPO}_4^{2-}}K_1$  ( $1.5(2) \times 10^3 \text{ M}^{-2} \text{ s}^{-1}$ ) can be obtained from the curve fit of the  $k_{\text{rxn}}$  vs  $\text{HPO}_4^{2-}$  plot.

**Steady-State Behavior of BrO<sub>2</sub><sup>-</sup>/SO<sub>3</sub><sup>2-</sup> Reaction Intermediates at  $p[\text{H}^+] 7.2\text{--}5.9$ .** Above  $p[\text{H}^+] 7.2$ , the  $\text{BrO}_2^-/\text{SO}_3^{2-}$  reaction rate has a first-order dependence in  $[\text{H}^+]$ . However below  $p[\text{H}^+] 7.2$ , the  $k_{\text{rxn}}$  values level off as  $[\text{H}^+]$  increases (Figure 4). This occurs in part because the fraction of protonated sulfite ion increases as  $[\text{H}^+]$  increases

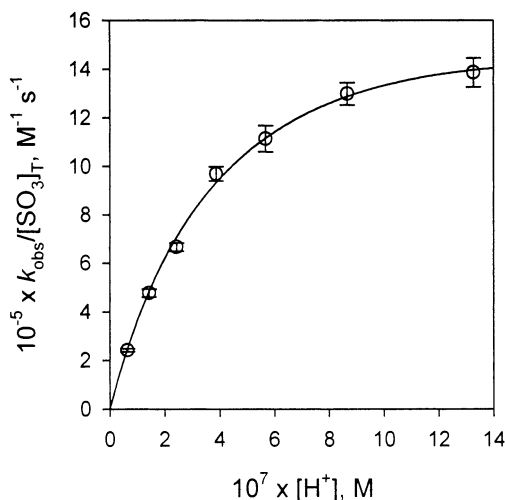


**Figure 4.**  $[\text{H}^+]$  dependence of bromite/sulfite reaction rate constant,  $k_{\text{obs}}/[\text{SO}_3]_{\text{T}}$  (o), at 0.106 mM  $\text{BrO}_2^-$ , 0.91–1.21 mM  $[\text{SO}_3]_{\text{T}}$ ,  $6.3 \times 10^{-8}\text{--}1.3 \times 10^{-6} \text{ M H}^+$ , and 30 mM  $[\text{PO}_4]_{\text{T}}$ . The solid line shows a curve fit to  $k_{\text{obs}}/[\text{SO}_3]_{\text{T}} = (d(e[\text{H}^+] + f[\text{H}^+][\text{H}_2\text{PO}_4^-])/d)/(1 + e[\text{H}^+] + f[\text{H}^+][\text{H}_2\text{PO}_4^-]/d)K_a(\text{SO}_3\text{H}^-)/(K_a(\text{SO}_3\text{H}^-) + [\text{H}^+])$ , where  $d = k_1 = 3.0(5) \times 10^7 \text{ M}^{-1} \text{ s}^{-1}$ ,  $e = k_4^{\text{H}_2\text{O}}K_2/k_{-1}K_w = 1.5(3) \times 10^5 \text{ M}^{-1}$ , and  $f = k_4^{\text{H}_2\text{PO}_4^-}K_1K_2/K_w = 1.3(3) \times 10^{13} \text{ M}^{-3} \text{ s}^{-1}$ . Error bars reflect the propagation of error in measurement.

( $pK_a(\text{SO}_3\text{H}^-) = 6.30$ ).<sup>23</sup> Under our experimental conditions, the rate of  $\text{SO}_3\text{H}^-$  reaction with  $\text{BrO}_2^-$  is negligible in comparison to the  $\text{BrO}_2^-/\text{SO}_3^{2-}$  reaction rate. However, this does not completely account for the rate behavior. Instead, these data show that as  $[\text{H}^+]$  increases the preequilibrium conditions are no longer valid and a steady-state approximation for the  $(\text{O}_2\text{BrSO}_3)^{3-}$  species is needed. The equation for the total steady-state concentrations ( $[\text{SS}]_{\text{T}}$ , eq 34)

$$[\text{SS}]_{\text{T}} = \frac{k_1[\text{BrO}_2^-][\text{SO}_3^{2-}](K_2 + [\text{OH}^-])}{k_{-1}[\text{OH}^-] + (k_3^{\text{H}_2\text{O}}[\text{OH}^-] + k_4^{\text{H}_2\text{O}}K_2 + k_4^{\text{H}_2\text{PO}_4^-}K_2[\text{H}_2\text{PO}_4^-])} \quad (34)$$

is derived by assuming that  $[\text{SS}]_{\text{T}}$  is equal to  $[(\text{O}_2\text{BrSO}_3)^{3-}] + [(\text{HO}_2\text{BrSO}_3)^{2-}]$ , and the ratio of the bromite/sulfite intermediates is related to  $K_2$  (eq 35). (A detailed derivation is given in the Supporting Information).

$$K_2 = \frac{[(\text{HO}_2\text{BrSO}_3)^{2-}][\text{OH}^-]}{[(\text{O}_2\text{BrSO}_3)^{3-}]} \quad (35)$$

The rate expression for bromite/sulfite reaction in the absence of buffers for  $p[\text{H}^+] < 7.2$  is shown in eq 36, where  $k_3^{\text{H}_2\text{O}}[\text{OH}^-]$  is negligible relative to  $k_4^{\text{H}_2\text{O}}K_2$ . The curve fit of the data (Figure 4) shows that  $k_1$ , which represents  $\text{BrO}_2^-/\text{SO}_3^{2-}$  direct reaction, is  $3.0(5) \times 10^7 \text{ M}^{-1} \text{ s}^{-1}$ . By comparison, sulfite reacts rapidly with hypohalous acids to form  $(\text{HOXS})_3^{2-}$  intermediates with rate constants of  $5.0 \times 10^9 \text{ M}^{-1} \text{ s}^{-1}$  for HOCl and HOBr.<sup>1c,1e</sup> Our data show that bromite is also very reactive but its rate constant is 2 orders of magnitude less. This indicates that  $\text{BrO}_2^-$  is a weaker electrophile than HOCl and HOBr.

$$\frac{k_{\text{obs}}}{[\text{SO}_3]_{\text{T}}} = \frac{k_1(k_4^{\text{H}_2\text{O}}K_2[\text{H}^+] + k_4^{\text{H}_2\text{PO}_4^-}K_2[\text{H}_2\text{PO}_4^-][\text{H}^+])}{k_{-1}K_w + k_4^{\text{H}_2\text{O}}K_2[\text{H}^+] + k_4^{\text{H}_2\text{PO}_4^-}K_2[\text{H}_2\text{PO}_4^-][\text{H}^+]} \times \frac{K_a(\text{SO}_3\text{H}^-)}{K_a(\text{SO}_3\text{H}^-) + [\text{H}^+]} \quad (36)$$

The  $[\text{H}^+]$  dependence of the  $\text{BrO}_2^-/\text{SO}_3^{2-}$  reaction rate below  $\text{p}[\text{H}^+] 7.2$  also provides further evidence that any  $\text{SO}_3\text{H}^-$  and  $\text{HBrO}_2$  reaction paths are negligible. The rate expressions for  $\text{BrO}_2^-/\text{SO}_3\text{H}^-$ ,  $\text{HBrO}_2/\text{SO}_3^{2-}$ , and  $\text{HBrO}_2/\text{SO}_3\text{H}^-$  reactions do not fit the data using known acid dissociation constants.

**Brønsted–Pedersen Relationship for the  $\text{BrO}_2^-/\text{SO}_3^{2-}$  Reaction.** General-acid-catalyzed reaction mechanisms often follow the Brønsted–Pedersen relationship,<sup>25a</sup> eq 37. This describes the correlation between the strength of the assisting acid in relation to the rate constant, where  $k^{\text{HA}}$  represents the composite general-acid-catalyzed rate constant,  $p$  is the number of equivalent acidic sites in HA,  $q$  is the number of equivalent basic sites in  $\text{A}^-$ ,  $G_a$  is a constant, and  $\alpha$  describes the sensitivity of the reaction to the acid strength of HA. Plots of the experimental data are shown in Figure 5. Both general-acid-catalyzed pathways (eqs 24 and 25) follow the Brønsted–Pedersen relation, where  $\alpha(k_3^{\text{HA}}K_1) = 0.88(7)$  and  $\alpha(k_4^{\text{HA}}K_1K_2/K_w) = 0.3(1)$ . This suggests there is a higher degree of proton transfer from HA to  $(\text{O}_2\text{BrSO}_3)^{3-}$  (Figure 6a) than to  $(\text{HO}_2\text{BrSO}_3)^{2-}$  (Figure 6b).

$$\log \frac{k^{\text{HA}}}{p} = \log G_a + \alpha \log \frac{qK_a}{p} \quad (37)$$

The behavior of boric acid is somewhat surprising because boric acid is a Lewis acid. However, Bell<sup>25b</sup> suggests that boric acid may act also as a Brønsted acid because it can coordinate a water to form a  $\text{H}_2\text{OB}(\text{OH})_3$  complex. This complex could donate a proton to the transition state.

**Lack of Buffer Dependence for the  $\text{ClO}_2^-/\text{S(IV)}$  Reaction.** The chlorite/S(IV) reaction shows no buffer dependence on the rate constant for 30–75 mM  $[\text{PO}_4]_{\text{T}}$  at  $\text{p}[\text{H}^+] 10.42(3)$ , 25–100 mM  $[\text{CO}_3]_{\text{T}}$  at  $\text{p}[\text{H}^+] 9.52(1)$ , 16–80 mM  $[\text{Bor}]_{\text{T}}$  at  $\text{p}[\text{H}^+] 8.75(2)$ , 125–200 mM  $[\text{PO}_4]_{\text{T}}$  at  $\text{p}[\text{H}^+] 6.38(1)$ , and 40–80 mM  $[\text{OAc}]_{\text{T}}$  at  $\text{p}[\text{H}^+] 4.33(5)$ . As the buffer concentration increases, the rate of reaction does not change. However, the rate increases with  $[\text{H}^+]$ . Thus, the acid dependence for the  $\text{ClO}_2^-/\text{S(IV)}$  reaction is due to specific-acid assistance, and not general-acid assistance.

**$[\text{H}^+]$  Dependence of the  $\text{ClO}_2^-/\text{S(IV)}$  Reaction.** The second-order rate constant for the reaction of chlorite with excess sulfite was measured as a function of  $[\text{H}^+]$  ( $\text{p}[\text{H}^+] 3.8$ – $11.1$ ). As  $[\text{H}^+]$  increases, an increase in the reaction rate is observed beginning near the  $\text{p}K_a$  value of  $\text{SO}_3\text{H}^-$ , which indicates that  $\text{SO}_3\text{H}^-$  is more reactive with  $\text{ClO}_2^-$  than  $\text{SO}_3^{2-}$ .

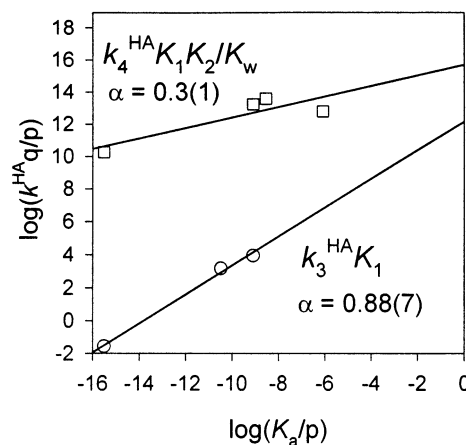


**Figure 5.** Brønsted–Pedersen plot for general-acid catalysis of  $\text{BrO}_2^-/\text{SO}_3^{2-}$  reaction:  $(\text{HO}_2\text{BrSO}_3)^{2-} + \text{HA}$  path ( $k_4^{\text{HA}}K_1K_2/K_w$ ) ( $\square$ ) and  $(\text{O}_2\text{BrSO}_3)^{3-} + \text{HA}$  path ( $k_3^{\text{HA}}K_1$ ) ( $\circ$ ). Data are fit to eq 37 where  $k^{\text{HA}}$  represents the composite rate constant for general-acid catalysis.

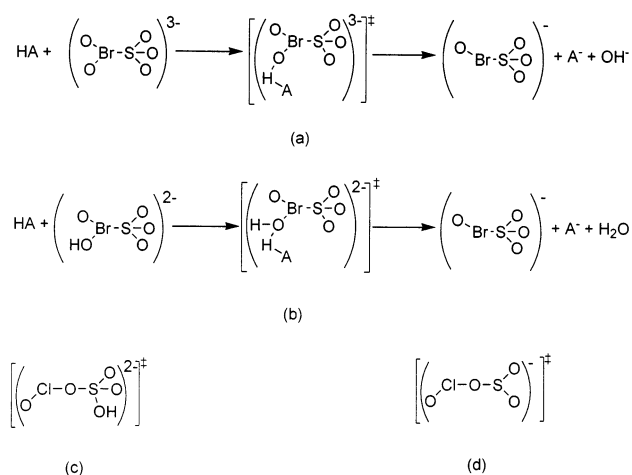


**Figure 6.** Proposed halite/S(IV) transition state species: (a)  $\text{BrO}_2^-/\text{SO}_3^{2-}/\text{HA}$  ( $k_3^{\text{HA}}K_1$  path, eq 24); (b)  $\text{BrO}_2^-/\text{SO}_3^{2-}/\text{HA}/\text{H}^+$  ( $k_4^{\text{HA}}K_1K_2/K_w$  path, eq 25); (c)  $\text{ClO}_2^-/\text{SO}_3\text{H}^-$  ( $k_6$  path, eq 42); (d)  $\text{ClO}_2^-/\text{SO}_2$  ( $k_5$  path, eq 41).

To obtain the rate parameters for this reaction, the data were fit in smaller  $\text{p}[\text{H}^+]$  ranges. The expression eq 38 is based on Frerichs' work<sup>9</sup> but includes the constant for  $\text{SO}_2/\text{SO}_3\text{H}^-$  equilibrium ( $\text{p}K_a(\text{SO}_2) = 1.90(5)$ ).<sup>23</sup> The best fit to the data occurs when the  $y$ -intercept ( $y_0$ ) value is zero. Since the  $y$ -intercept represents direct chlorite/sulfite reaction, this indicates that the direct reaction between  $\text{ClO}_2^-$  and  $\text{SO}_3^{2-}$  is negligible.

$$\frac{k_{\text{obs}}}{[\text{SO}_3]_{\text{T}}}([\text{H}^+]^2 + K_a(\text{SO}_2)[\text{H}^+] + K_a(\text{SO}_3\text{H}^-)K_a(\text{SO}_2)) = y_0 + a[\text{H}^+] + b[\text{H}^+]^2 \quad (38)$$

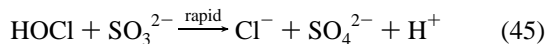
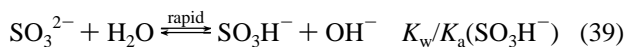
A plot of  $k_{\text{rxn}}$  vs  $\text{p}[\text{H}^+]$  is shown in Figure 7. The data fit the rate expression generated by eq 38 where  $a = 5.7(3) \times 10^{-2} \text{ s}^{-1}$  and  $b = 6.26(4) \times 10^6 \text{ M}^{-1} \text{ s}^{-1}$ . No higher order paths were found (such as  $[\text{H}^+]^3$ ), which shows that, for  $\text{p}[\text{H}^+] > 3.8$ , the contribution of  $\text{HClO}_2$  ( $\text{p}K_a = 1.72$ )<sup>26</sup> to the reaction rate constant can be neglected.

(25) Bell, R. P. *The Proton in Chemistry*, 2nd ed.; Cornell University: Ithaca, NY, 1973; (a) pp 195–198, (b) p 223, (c) p 200.

(26) Fabian, I.; Gordon, G. *Inorg. Chem.* **1992**, *31*, 2144–2150.

**ClO<sub>2</sub><sup>-</sup>/S(IV) Reaction Mechanism.** The mechanism for the ClO<sub>2</sub><sup>-</sup>/S(IV) reaction must include several features that are different from the BrO<sub>2</sub><sup>-</sup>/S(IV) mechanism but are required by the kinetics. No ClO<sub>2</sub><sup>-</sup>/SO<sub>3</sub><sup>2-</sup> direct reaction is observed because the y-intercept for the plot of  $k_{\text{obs}}/[\text{SO}_3]_{\text{T}}$  vs  $[\text{H}^+]$  is zero. Although the ClO<sub>2</sub><sup>-</sup>/SO<sub>3</sub><sup>2-</sup> reaction potential is slightly more favorable than the BrO<sub>2</sub><sup>-</sup>/SO<sub>3</sub><sup>2-</sup> reaction potential, the ClO<sub>2</sub><sup>-</sup>/SO<sub>3</sub><sup>2-</sup> reaction rate is negligible whereas the BrO<sub>2</sub><sup>-</sup>/SO<sub>3</sub><sup>2-</sup> reaction rate constant is  $3.0 \times 10^7 \text{ M}^{-1} \text{ s}^{-1}$ . Instead, ClO<sub>2</sub><sup>-</sup> reacts preferentially with SO<sub>3</sub>H<sup>-</sup>, while the BrO<sub>2</sub><sup>-</sup>/SO<sub>3</sub>H<sup>-</sup> reaction is negligible. Furthermore, if the ClO<sub>2</sub><sup>-</sup>/S(IV) reaction mechanism were the same as the BrO<sub>2</sub><sup>-</sup>/S(IV) reaction mechanism, we would expect strong general-acid catalysis of the reaction rate by reaction with ClO<sub>2</sub><sup>-</sup>/SO<sub>3</sub><sup>2-</sup> and ClO<sub>2</sub><sup>-</sup>/SO<sub>3</sub>H<sup>-</sup> intermediates. However, buffers have no effect on the reaction rate. These distinctions require a mechanism for the ClO<sub>2</sub><sup>-</sup>/S(IV) reaction that is fundamentally different from the BrO<sub>2</sub><sup>-</sup>/S(IV) reaction.

The mechanism of eqs 39–45 is developed on the basis of the experimental data, where ClO<sub>2</sub><sup>-</sup> acts as a nucleophile and SO<sub>2</sub> and SO<sub>3</sub>H<sup>-</sup> are electrophiles. Sulfite is in a rapid preequilibrium with hydrogen sulfite, which is in rapid preequilibrium with sulfur dioxide. Chlorite and sulfur dioxide react to form an intermediate (OCIOSO<sub>2</sub>)<sup>-</sup>, which rapidly dissociates into OCl<sup>-</sup> and SO<sub>3</sub>. The hydrolysis of the SO<sub>3</sub> product is rapid in aqueous solution.<sup>27</sup> Similarly, chlorite and hydrogen sulfite react to form an (OCIOSO<sub>3</sub>H)<sup>2-</sup> intermediate, which rapidly dissociates into OCl<sup>-</sup> and HOSO<sub>3</sub><sup>-</sup>. OCl<sup>-</sup> is in rapid equilibrium with HOCl ( $K_{\text{a}}(\text{HOCl}) = 10^{-7.47} \text{ M}$ ),<sup>1d</sup> and HOCl is rapidly reduced to Cl<sup>-</sup> by a second SO<sub>3</sub><sup>2-</sup> ( $k = 7.6 \times 10^8 \text{ M}^{-1} \text{ s}^{-1}$ )<sup>1c</sup>.



Hydrogen sulfite exists in two isomeric forms: HSO<sub>3</sub><sup>-</sup>, where the proton is bonded to the sulfur, and HOSO<sub>2</sub><sup>-</sup>, where the proton is bonded to an oxygen. The latter isomer predominates, and the ratio  $K^{\text{S}} = [\text{HOSO}_2^-]/[\text{HSO}_3^-]$  is 4.9 at 25.0 °C,  $\mu = 1.0 \text{ M}$ .<sup>28</sup> We expect only the HOSO<sub>2</sub><sup>-</sup> isomer to be reactive because a chlorite to sulfur bond is needed for the reaction mechanism. Since  $k_6$  refers to the average rate constant for the two isomeric forms of hydrogen sulfite,

(27) Meijer, E. J.; Sprik, M. *J. Phys. Chem. A* **1998**, *102*, 2893–2898.

(28) Horner, D. A.; Connick, R. E. *Inorg. Chem.* **1986**, *25*, 2414–2417.

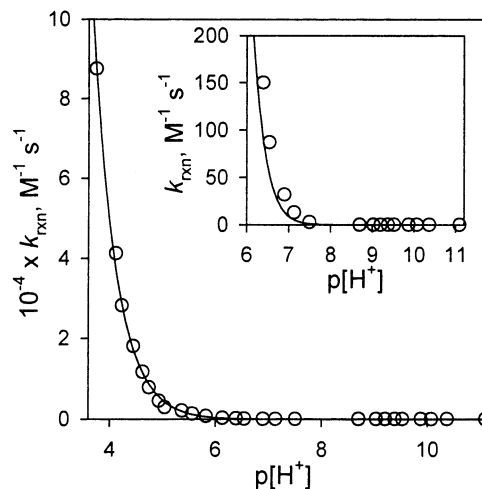


**Figure 7.**  $\text{p}[\text{H}^+]$  dependence of chlorite/S(IV) rate constant ( $k_{\text{rxn}}$ , o). Solid line (—) fits the following equation:  $k_{\text{rxn}} = (5.7 \times 10^{-2}[\text{H}^+] + 6.26 \times 10^6[\text{H}^+]^2)/([\text{H}^+]^2 + K_{\text{a}}(\text{SO}_2)[\text{H}^+] + K_{\text{a}}(\text{SO}_3\text{H}^-)K_{\text{a}}(\text{SO}_2))$ . The insert shows the increase in rate constant near  $\text{p}K_{\text{a}}(\text{SO}_3\text{H}^-)$ . Conditions:  $\mu = 1.0 \text{ M}$ ; 25.0(1) °C.

the rate parameter must be corrected for the HSO<sub>3</sub><sup>-</sup> isomer. The rate expression for the ClO<sub>2</sub><sup>-</sup>/SO<sub>3</sub>H<sup>-</sup> reaction mechanism is shown in eq 46, and the resolved rate constants, obtained from the fit of eq 38, are  $b = k_5 = 6.26(4) \times 10^6 \text{ M}^{-1} \text{ s}^{-1}$  and  $a(1 + K^{\text{S}})/(K^{\text{S}}K_{\text{a}}(\text{SO}_2)) = k_6 = 5.5(3) \text{ M}^{-1} \text{ s}^{-1}$ .

$$\frac{k_{\text{obs}}}{[\text{SO}_3]_{\text{T}}} = \frac{k_5[\text{H}^+]^2 + k_6 \left( \frac{K^{\text{S}}K_{\text{a}}(\text{SO}_2)}{1 + K^{\text{S}}} \right) [\text{H}^+]}{([\text{H}^+]^2 + K_{\text{a}}(\text{SO}_2)[\text{H}^+] + K_{\text{a}}(\text{SO}_3\text{H}^-)K_{\text{a}}(\text{SO}_2))} \quad (46)$$

The rate constant for ClO<sub>2</sub><sup>-</sup>/SO<sub>2</sub> reaction ( $k_5$ ) is 6 orders of magnitude larger than ClO<sub>2</sub><sup>-</sup>/SO<sub>3</sub>H<sup>-</sup> rate constant ( $k_6$ ). The SO<sub>2</sub> path predominates when  $\text{p}[\text{H}^+] < 7.5$ . SO<sub>2</sub> is a much better electrophile than SO<sub>3</sub>H<sup>-</sup>, and the rate constant for reaction with chlorite, a nucleophile, increases with increasing electrophilicity of S(IV). A similar behavior has been observed for bromate/S(IV) reaction, where the BrO<sub>3</sub><sup>-</sup>/SO<sub>2</sub> rate constant is 3100 times greater than the BrO<sub>3</sub><sup>-</sup>/SO<sub>3</sub>H<sup>-</sup> rate constant.<sup>29</sup>

An alternate mechanism was also considered (see Supporting Information). This mechanism includes chlorite and hydrogen sulfite in a rapid preequilibrium with a (OCIOSO<sub>3</sub>H)<sup>2-</sup> intermediate. This intermediate would protonate, which allows for the observed squared  $[\text{H}^+]$  dependence. Both intermediates would dissociate in the rate-determining steps to form OCl<sup>-</sup> and HOSO<sub>3</sub><sup>-</sup>. The  $[\text{H}^+]$  dependence for this mechanism is identical to the mechanism given in eqs 39–45 under our conditions. Thus, the mechanisms are kinetically indistinguishable. However, we prefer the mechanism given in eqs 39–45 because it accounts for the expected electrophilicity difference between SO<sub>2</sub> and SO<sub>3</sub>H<sup>-</sup>. SO<sub>2</sub> is more electrophilic than SO<sub>3</sub>H<sup>-</sup>, and SO<sub>2</sub> reacts faster with ClO<sub>2</sub><sup>-</sup> than SO<sub>3</sub>H<sup>-</sup>.

**Oxygen-Atom Transfer vs Oxyhalogen Transfer.** The proposed BrO<sub>2</sub><sup>-</sup>/S(IV) reaction mechanism includes inter-

(29) Szivoczka, L.; Boga, E. *Int. J. Chem. Kinet.* **1998**, *30*, 869–874.



mediates with Br–S connectivity rather than O–S connectivity.  $\text{BrO}_2^-$  acts as an electrophile in this reaction, and the Br atom expands its octet to accept an electron pair from the nucleophilic sulfur atom of  $\text{SO}_3^{2-}$ . General acids assist the removal of an oxide ion from  $(\text{O}_2\text{BrSO}_3)^{3-}$  (Figure 6a) or a hydroxide ion from  $(\text{HO}_2\text{BrSO}_3)^{2-}$  (Figure 6b). If general acids did not remove the oxide or hydroxide from the bromine side of the intermediate, incorrect products would form. The data analysis shows that the rate of the  $\text{BrO}_2^-/\text{S(IV)}$  reaction decreases as the fraction of protonated  $[\text{SO}_3]_{\text{T}}$  increases. Protonation of  $\text{SO}_3^{2-}$  reduces the nucleophilicity of the S atom and reduces the fraction of  $(\text{O}_2\text{BrSO}_3)^{3-}$  formed.

The alternative connectivities of  $(\text{BrO}_2\cdot\text{SO}_3)^{3-}$  contain O–S bonds:  $(\text{O}_2\text{BrOSO}_2)^{3-}$  and  $(\text{OBrOSO}_3)^{3-}$ . The  $(\text{O}_2\text{BrOSO}_2)^{3-}$  species does not provide a path that leads to the products so it can be ruled out. The  $(\text{OBrOSO}_3)^{3-}$  species is conceivable as an oxygen-atom transfer from bromine to sulfur, which would give  $\text{OBr}^-$  and  $\text{SO}_4^{2-}$ . However, there is no obvious way that general acids would catalyze the decomposition of  $(\text{OBrOSO}_3)^{3-}$ . If HA reacts with the oxybromine side of the intermediate, then the HA would remove an  $\text{OBr}^-$  so that the oxygen atom could be transferred to the sulfur. This is not a characteristic general acid function. Instead, general acids typically react with  $\text{O}^{2-}$  or  $\text{OH}^-$  to form  $\text{OH}^-$  or  $\text{H}_2\text{O}$ . HA could react with the sulfur side of the halite/S(IV) intermediate. This would result in an  $(\text{OBrOSO}_2)^-$  intermediate that would have to hydrolyze at the sulfur to produce  $\text{OBr}^-$  and  $\text{HOSO}_3^-$ . It is illogical that the function of the general acid is to remove the  $\text{OH}^-$  in the first step, only to have it return in the subsequent steps. In fact, the general acid reaction is completely unnecessary to produce  $\text{OBr}^-$  and  $\text{HOSO}_3^-$  from  $(\text{OBrOSO}_3\text{H})^{2-}$ . Of the possible  $(\text{BrO}_2\cdot\text{SO}_3)^{3-}$  connectivities, only the adduct with Br–S bonds requires general-acid catalysis. For these reasons, we use the general-acid catalysis as the rationale for the Br–S connectivity of the bromite/sulfite intermediates.

The  $\text{ClO}_2^-/\text{S(IV)}$  reaction mechanism includes intermediates with O–S connectivity rather than Cl–S connectivity. This reaction shows a specific-acid, not a general-acid, catalysis. The Cl atom does not expand its octet as easily as the Br atom and cannot accept the electrons from sulfur as easily as the Br atom. Furthermore, the Cl–O bond is less polar than the Br–O bond. Therefore, the Cl atom in  $\text{ClO}_2^-$  is not as electropositive as the Br atom in  $\text{BrO}_2^-$  and is not a good electrophile. To overcome this,  $\text{ClO}_2^-$  reacts through the O atom, which is more nucleophilic. As a consequence,  $\text{ClO}_2^-$  acts as a nucleophile and reacts preferentially with  $\text{SO}_2$  and  $\text{SO}_3\text{H}^-$ , which are better electrophiles than  $\text{SO}_3^{2-}$ .  $\text{SO}_2/\text{SO}_3\text{H}^-$  and  $\text{ClO}_2^-$  form adducts with expanded valence around the S atom via oxygen/sulfur connectivity (Figure 6c,d). These adducts,  $(\text{OCIOSO}_2)^-$  and  $(\text{OCIOSO}_3\text{H})^{2-}$ , form  $\text{OCl}^-$  and  $\text{HOSO}_3^-$ . If the  $\text{ClO}_2^-/\text{S(IV)}$  mechanism were the same as the  $\text{BrO}_2^-/\text{S(IV)}$  mechanism, then we would expect intermediates with Cl–S connectivity that would react with general acids. However, the lack of general-acid catalysis shows that the  $\text{ClO}_2^-/\text{S(IV)}$  mechanism prefers intermediates

with O–Cl connectivity, which do not have to react with general acids.

The thermodynamic driving forces for the  $\text{BrO}_2^-/\text{SO}_3^{2-}$  and  $\text{ClO}_2^-/\text{SO}_3^{2-}$  reactions are comparable. Yet, the  $\text{ClO}_2^-/\text{S(IV)}$  reaction is more than 5 orders of magnitude slower than the  $\text{BrO}_2^-/\text{S(IV)}$  reaction in basic solution. The  $\text{ClO}_2^-/\text{S(IV)}$  reaction must overcome significant kinetic barriers for reaction to occur. The proposed reaction mechanism proceeds through  $(\text{OCIOSO}_3\text{H})^{2-}$  and  $(\text{OCIOSO}_2)^-$  intermediates, where chlorite donates an electron pair to sulfur. Sulfur can expand its number of valence electrons more readily than oxygen. The rate-determining steps for the  $\text{ClO}_2^-/\text{S(IV)}$  reaction include oxidation of the sulfur atom, transfer of an oxygen atom, and reduction of the chlorine atom (eq 47).



If only the dependence in  $[\text{H}^+]$  were considered, it may be reasonable to assume that the  $\text{BrO}_2^-/\text{S(IV)}$  reaction and the  $\text{ClO}_2^-/\text{S(IV)}$  reaction occur through the same oxygen-atom transfer mechanism. However, rate expressions that include  $\text{SO}_3\text{H}^-$  or  $\text{SO}_2$  reaction with  $\text{BrO}_2^-$  do not fit the data (using known values the acid dissociation constants). Furthermore, the observed general-acid catalysis of the  $\text{BrO}_2^-/\text{S(IV)}$  reaction and the lack of a general-acid catalysis for the  $\text{ClO}_2^-/\text{S(IV)}$  reaction shows that the  $\text{BrO}_2^-/\text{S(IV)}$  intermediates must have a different connectivity than the  $\text{ClO}_2^-/\text{S(IV)}$  intermediates. General-acid catalysis is required for  $(\text{O}_2\text{BrSO}_3)^{3-}$  to produce  $\text{OBr}^-$  and  $\text{SO}_4^{2-}$ , while a general-acid catalysis is not needed for  $(\text{OCIOSO}_3\text{H})^{2-}$  to produce  $\text{OCl}^-$  and  $\text{OSO}_3\text{H}^-$ . For these reasons, we cannot assign the  $\text{BrO}_2^-/\text{S(IV)}$  reaction the same mechanism as the  $\text{ClO}_2^-/\text{S(IV)}$  reaction.

In comparison of chlorite/sulfite and bromite/sulfite reaction mechanisms, it is known that the reactions of hypochlorous acid and hypobromous acid with sulfite occur through halogen–sulfur intermediates.<sup>1c,1e,30</sup> Others have studied the kinetics and mechanisms of bromate/S(IV) reaction<sup>29,31</sup> and chlorate/S(IV) reaction.<sup>32–34</sup> The reaction rates of these halates increase as  $[\text{SO}_3]_{\text{T}}$  becomes more protonated. Despite favorable thermodynamics (eqs 48 and 49),<sup>10,11</sup> bromate and chlorate show virtually no reaction with  $\text{SO}_3^{2-}$ . Furthermore, the bromate/S(IV) reaction rate is not affected by buffers,<sup>31</sup> which is similar to the chlorite/S(IV) kinetics. In light of these observations, we propose that, for S(IV)/oxyhalogenate reactions, reductions of Cl(III), Cl(V), and Br(V) proceed by oxygen/sulfur intermediates, while Br(III), Br(I), and Cl(I) prefer halogen/sulfur intermediates. The arrangement of the oxyhalogen/S(IV) intermediate and whether the oxyhalogen anion acts as a nucleophile or electrophile relative to S(IV) determines the reaction rate. We propose that the

(30) Yiin, B. S.; Margerum, D. W. *Inorg. Chem.* **1988**, *27*, 1670–1672.

(31) Williamson, F. S.; King, E. L. *J. Am. Chem. Soc.* **1957**, *79*, 5397–5400.

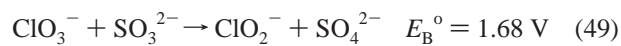
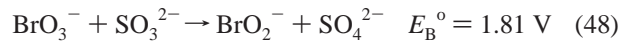
(32) Gleason, E. H.; Mino, G.; Thomas, W. M. *J. Am. Chem. Soc.* **1957**, *61*, 447–450.

(33) Dobrynin, N. A.; Dymarchuk, N.; P.; Mishchenko, K. P. *Zh. Obshch. Khim.* **1969**, *39*, 2157–2164.

(34) Menéndez, S. M. *Rev. Fac. Cienc.* **1968**, *9*, 119–213.

#### *S(IV) Reductions of Bromite and Chlorite Ions*

presence or absence of general-acid catalysis and the oxyhalogen reactivity toward  $\text{SO}_3^{2-}/\text{SO}_3\text{H}^-$  is a consequence of the connectivity of the oxyhalogen/S(IV) reaction intermediate.



**Acknowledgment.** This work was supported by National Science Foundation Grants CHE-9818214 and CHE-0139876

and an Emerson Kampen Foundation Fellowship to Purdue University (K.E.H.H.).

**Supporting Information Available:** Tables and figures of kinetic data, the derivation of the rate expression derivation for  $\text{BrO}_2^-/\text{SO}_3^{2-}$  reaction, an alternative mechanism for  $\text{ClO}_2^-/\text{S(IV)}$  reaction, and a description of polyborate distribution calculation. This material is available free of charge via the Internet at <http://pubs.acs.org>.

IC020475M